JOURNAL OF GEOPHYSICAL RESEARCH, VOL. 102, NO. C9, PAGES 21,115–21,129, SEPTEMBER 15, 1997

Inertial dissipation method applied to derive turbulent fluxes over the ocean during the Surface of the Ocean, Fluxes and Interactions with the Atmosphere/Atlantic Stratocumulus Transition Experiment (SOFIA/ASTEX) and Structure des Echanges Mer-Atmosphere, Proprietes des Heterogeneites Oceaniques: Recherche Experimentale (SEMAPHORE) experiments with low to moderate wind speeds

Hélène Dupuis,[1] Peter K. Taylor,[2] Alain Weill,[1] and K. Katsaros[3]

Abstract. The transfer coefficients for momentum and heat have been determined for 10 m neutral wind speeds (U_{10n}) between 0 and 12 m/s using data from the Surface of the Ocean, Fluxes and Interactions with the Atmosphere (SOFIA) and Structure des Echanges Mer-Atmosphere, Proprietes des Heterogeneites Oceaniques: Recherche Experimentale (SEMAPHORE) experiments. The inertial dissipation method was applied to wind and pseudo virtual temperature spectra from a sonic anemometer, mounted on a platform (ship) which was moving through the turbulence field. Under unstable conditions the assumptions concerning the turbulent kinetic energy (TKE) budget appeared incorrect. Using a bulk estimate for the stability parameter, Z/L (where Z is the height and L is the Obukhov length), this resulted in anomalously low drag coefficients compared to neutral conditions. Determining Z/L iteratively, a low rate of convergence was achieved. It was concluded that the divergence of the turbulent transport of TKE was not negligible under unstable conditions. By minimizing the dependence of the calculated neutral drag coefficient on stability, this term was estimated at about $-0.65Z/L$. The resulting turbulent fluxes were then in close agreement with other studies at moderate wind speed. The drag and exchange coefficients for low wind speeds were found to be $C_{en} \times 10^3 = 2.79U_{10n}^{-1} + 0.66$ ($U_{10n} < 5.2$ m/s), $C_{en} \times 10^3 = C_{hn} \times 10^3 = 1.2$ ($U_{10n} \geq 5.2$ m/s), and $C_{dn} \times 10^3 = 11.7U_{10n}^{-2} + 0.668$ ($U_{10n} < 5.5$ m/s), which imply a rapid increase of the coefficient values as the wind decreased within the smooth flow regime. The frozen turbulence hypothesis and the assumptions of isotropy and an inertial subrange were found to remain valid at these low wind speeds for these shipboard measurements. Incorporation of a free convection parameterization had little effect.

1. Introduction

Only experimental results with direct or indirect flux estimates can provide the drag and exchange coefficients needed to derive turbulent fluxes at the air-sea interface from bulk meteorological measurements. Several uncertainties remain concerning these drag and exchange coefficients, for example, the correct values for high wind regimes and the effects of varying sea state. Parameterization at low wind speeds is also a crucial point. An illustration of this problem is given by the Tropical Ocean-Global Atmosphere Coupled Ocean-Atmosphere Response Experiment (TOGA COARE) warm pool area, where very long periods of low wind speeds occur for which heat fluxes must be accurately parameterized in connection with the convection in the lower atmosphere. Light wind conditions are also often observed in the extratropical high-pressure region of the midlatitude North Atlantic; this paper will make use of low wind speed data from two air-sea interaction experiments in that region.

In order to better establish drag or exchange coefficients at low wind speeds (or, equivalently, the roughness lengths, z_0, z_t, and z_q for wind speed, air temperature, and humidity), good quality estimates of the friction velocity, u^*, are needed at low wind speeds. Consideration of the physics and dimensional analysis suggests that the parameterizations would best be formulated in terms of the roughness lengths. However, although the transfer coefficients can be deduced from the roughness lengths and vice versa, the relationships are nonlinear, and a mean value for the transfer coefficient does not necessarily correspond to the mean roughness length. In practical applications it is the transfer coefficients which are required in order to determine the fluxes from mean meteorological measurements. Therefore, in this paper we have chosen to determine parameterizations for the mean transfer coefficients. Although the similarity regime within a viscous sublayer leads to the enhancement of the drag coefficient with the wind speed

[1]Centre d'Etudes des Environnements Terrestres et Planétaires, Centre National de la Recherche Scientifique, Velizy, France.
[2]James Rennell Division for Ocean Circulation, Southampton Oceanography Centre, Southampton, England.
[3]Institut Français de la Recherche sur la Mer, Plouzané, France.

Copyright 1997 by the American Geophysical Union.

Paper number 97JC00446.
0148-0227/97/97JC-00446$09.00

below a certain threshold (associated with the aerodynamically smooth flow for which $z_0 \propto 1/u^*$ instead of $z_0 \propto u^{*2}$ as for rougher flows), neither the magnitude of the threshold nor the magnitude of the corresponding drag coefficients has been accurately established from experimental studies.

The inertial dissipation technique is a very convenient method to derive turbulent fluxes at the air-sea interface and hence has provided the drag and exchange coefficients used in most global studies of oceanography or meteorology. Its convenience is due to the fact that estimates of the momentum and heat fluxes can be derived without knowledge of the motion of the measuring platform. This method can therefore be used within a wide range of meteorological conditions. However, it is an indirect method, and one must prove its validity in all conditions. The technique has recently been reevaluated by several authors. While a good agreement was found in previous studies with the direct, eddy-correlation method [*Large and Pond*, 1981, 1982; *Edson et al.*, 1991], other studies have shown inconsistencies between the two methods for unstable stratification and/or low wind speed [*Bradley et al.*, 1991; *Greenhut and Khalsa*, 1995; *Dupuis et al.*, 1995] or particular sea states [*Donelan et al.*, 1997]. Apart from the difficulty of using the eddy-correlation method over the sea, these discrepancies may be associated with the hypotheses underlying the inertial dissipation method. For example, likely problem areas are anisotropy of the turbulence in the inertial subrange or existence of an $f^{-5/3}$ spectral shape [*Neugum*, 1996] and the assumptions regarding the turbulent kinetic energy budget [*Dupuis et al.*, 1995; *Yelland and Taylor*, 1996] (hereinafter referred to as DWKT95 and YT96).

Two experiments were recently performed in the Azores region, Surface of the Ocean, Fluxes and Interactions with the Atmosphere/Atlantic Stratocumulus Transition Experiment (SOFIA/ASTEX) in June 1992 and Structure des Echanges Mer-Atmosphere, Proprietes des Heterogeneites Oceaniques: Recherche Experimentale (SEMAPHORE) in October–November 1993. Turbulent measurements of wind speed were recorded using a sonic anemometer situated above the foredeck of a research vessel. Since the sensor motion was not measured, only the inertial dissipation technique can be used to derive the momentum flux or friction velocity. As described in DWKT95, low wind speeds were encountered during these two experiments with sea-air temperature differences varying between 0°C and 4°C. A preliminary analysis of these data (DWKT95) revealed several problems with the inertial dissipation method for unstable stratification. In particular, the calculated "neutral" values for the drag coefficients were dependent on the stability with much lower values at unstable stratification for a given wind speed compared to the near-neutral data. Also using a classical inertial dissipation method [e.g., *Large and Pond*, 1981, 1982], the calculated neutral drag coefficients, C_{dn}, were found to be much lower on average than in previous studies. We will assume that because of the dependence of the C_{dn} values on the stratification this discrepancy was mainly due to the parameterization of the different terms in the budget of turbulent kinetic energy (TKE), on which the method is based. In this paper, following a short description of the experiments, we will consider this point in a section discussing the inertial dissipation method. Then the results will be discussed with regard to the parameterization of the TKE budget and the resulting drag and exchange coefficients, with emphasis on wind speeds below 5 m/s. For these light winds the approach proposed by *Beljaars* [1995] to account for the gustiness factor associated with convection has been applied in order to better match free convection limits. The validity of the flux estimates at very low wind speeds will be discussed, based on the verification of assumptions underlying the inertial dissipation method (the Taylor hypothesis, the local isotropy hypothesis, and the spectral shape in the inertial subrange). Finally, the influence of surface current will be considered.

2. Description of the Experiments

This paper is based on data recorded during SOFIA/ASTEX and SEMAPHORE experiments. These two campaigns took place in June 1992 and October–November 1993, respectively, south of the Azores (in the North Atlantic, in open and deep ocean). In particular, SOFIA/ASTEX and SEMAPHORE were devoted to air-sea interaction studies. *Weill et al.* [1995] and *Eymard et al.* [1996] give a general overview of the aims and strategy of the two experiments. This particular study concerns the qualification and parameterization of turbulent fluxes at the air-sea interface, for which an instrumented mast was mounted on the foredeck of a research vessel, *Le Suroit*. Mean meteorological sensors were used (during SEMAPHORE, for example, instruments included Vaisala capacitance humidity and temperature probes, two-cup anemometers (R. M. Young Company), a pressure sensor, and also a thermosalinograph providing the sea surface temperature (SST) at about 2.5 m below the sea surface). Two systems provided the ship's velocity and direction: first, the electromagnetic log which provides the ship velocity relative to the near surface water and, second, the Global Positioning System (GPS) which provides the velocity relative to the seabed. For interpretation of the wind stress data the velocity relative to the water is required. However, since it is very difficult to obtain an accurate calibration for an electromagnetic log which is valid at the very low ship speeds typical of research ships, the values from the GPS system have been used. It is suggested that the errors due to neglecting surface currents would be smaller than the errors inherent in the electromagnetic log values; this will be further discussed in section 5. Turbulence measurements included a sonic anemometer, mounted at the top of the mast, corresponding to a height of 16 m for SOFIA and 16.5 m for SEMAPHORE above the sea surface. This sonic anemometer is an omnidirectional version of the solent sonic anemometer (manufactured by Gill Instruments), which can be sampled either at 56 Hz or 21 Hz, with measurements of six propagation times for sound pulses between the transducers or speeds for three wind components and also the speed of sound (u, v, w, c), respectively.

To estimate the dissipation rates of wind and thermal energy, fast Fourier transforms of the different parameters provided by the sonic anemometer were computed over 2^{14} samples (about 13 min) every 15 min. In order to reduce the quantity of data, only the average of the product of power spectral density and the frequency to the 5/3 power ($\langle E(f) f^{5/3} \rangle$) were recorded for specified frequency bands which were assumed to be within the inertial subrange. This assumption has been checked by examining the power laws for the spectral densities within the frequency bands, which were also recorded. During SOFIA/ASTEX the spectra were computed in real time; one fixed frequency band was considered (2–4 Hz), and only the downwind energy dissipation rates were calculated.

During SEMAPHORE the spectra were computed after the

experiment, and dissipation rates have been estimated for the energy of the downwind, cross-wind, and vertical wind component and the virtual temperature. For example, Figure 1 shows spectra of the wind energy for the downwind and vertical wind components. Comparison of the dissipation rates for the three wind speed components has allowed validation of the basic assumptions associated with the inertial dissipation method (i.e., the existence of an inertial subrange and the local isotropy). Three fixed frequency bands (0.5–1, 1–3, and 2–4 Hz) were used; these are shown by the horizontal solid lines in Figure 1. The dissipation rates were derived from a hierarchical test in which the band selected was the highest frequency band whose power law corresponded, within 10%, to −5/3. On the basis of this criterion, in the example shown in Figure 1, all three bands lie within the inertial subrange. The hierarchical test was designed to favor frequencies away from the spectral peak, located at around 10^{-1} Hz (see Figure 1), which was related to the ship motion. In fact, this test led, in most cases, to the selection of the highest frequency band, 2–4 Hz, while the lower frequency band (0.5–1 Hz) was never selected. Thus, in practice, the dissipation rate computations for SOFIA and SEMAPHORE data were similar, normally using the same frequency band. The selection criterion led to the rejection of several samples, mostly from temperature spectra whose high-frequency noise is a significant limitation.

The whole data set represents 951 runs of 13 min. In section 3 the inertial dissipation method describes in detail how the wind and sound speed spectra derived from the sonic anemometer were used to provide momentum and turbulent heat fluxes.

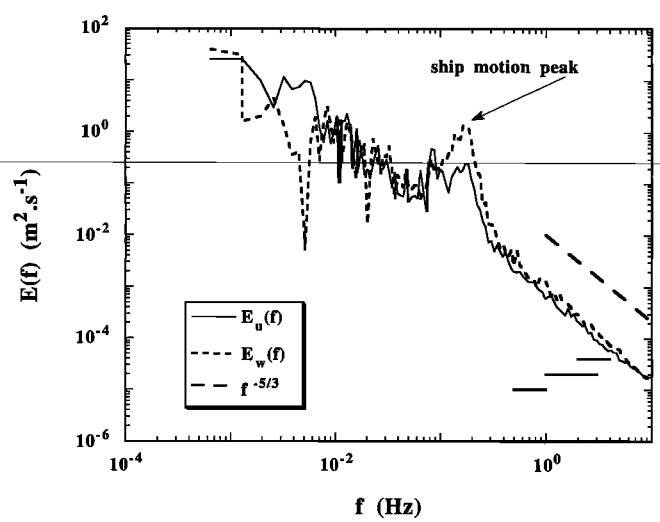

Figure 1. Power spectral density of the downwind ($E_u(f)$, solid line) and vertical wind ($E_w(f)$, short dashed line) components during the SEMAPHORE experiment on November 13, 1993, at 1000 UT. The spectra have been averaged into 150 log-spaced samples in order to reduce the variability of spectral densities and therefore to show the main features. They correspond to very low mean wind speed conditions (about 1 m/s). As a reference, the −5/3 power law for the inertial subrange is displayed with the dashed line. The three fixed frequency bands of 0.5–1, 1–3, and 2–4 Hz are shown with horizontal solid lines.

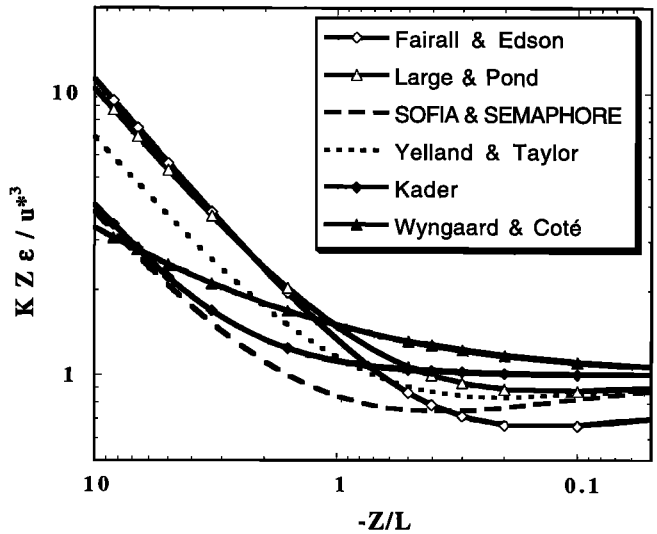

Figure 2. Summary of the different parameterizations of the TKE budget as a function of Z/L, as found in the literature [*Fairall and Edson*, 1994; *Large and Pond*, 1981; YT96; *Kader*, 1992; *Wyngaard and Coté*, 1971]. The parameterization derived later in this study is labeled SOFIA & SEMAPHORE.

3. Inertial Dissipation Method

3.1. Background

For the momentum flux this method is based on the budget of turbulent kinetic energy. In a stationary, horizontally homogeneous surface layer the balance for the TKE takes the form

$$0 = \Phi_m(Z/L) - Z/L - \frac{\kappa Z}{u^{*3}}\frac{\partial\langle we\rangle}{\partial z} - \frac{\kappa Z}{u^{*3}}\frac{\partial}{\partial z}\frac{\langle wp\rangle}{\rho} - \frac{\kappa Z}{u^{*3}}\varepsilon \tag{1}$$

where terms 1 and 2 correspond to the shear and the buoyant production (or loss), respectively. Because the TKE equation is shown in a nondimensional form, these terms appear as the stratification function, Φ_m, and the ratio of the height of measurement, Z, to the Monin-Obukhov length, L. The dissipation rate ε is deduced from the spectral energy of the wind velocity in the inertial subrange, assuming local isotropy. The turbulent transport and pressure correlation terms 3 and 4 cannot easily be determined independently and will therefore be denoted as an imbalance function, $\Phi_{\mathrm{imb}}(Z/L)$ in the following, corresponding to the sum of two transport terms. The sum can be deduced if the dissipation rate and a direct estimate of the friction velocity u^* are measured. However, direct estimation of u^* using the eddy-correlation technique is not an easy task from a moving platform over the ocean since corrections due to the platform are several orders higher than the fluctuations. Measurements over land (Kansas) or by aircraft [*Lenschow*, 1974] are available from experimental campaigns, but large errors in each of the different terms led to great uncertainties in the imbalance. Let us denote term 5, deduced from the sum of all other terms in (1) by $\Phi_\varepsilon(Z/L)$, thus

$$\Phi_\varepsilon(Z/L) = \frac{\kappa Z}{u^{*3}}\varepsilon = \Phi_m(Z/L) - Z/L - \Phi_{\mathrm{imb}}(Z/L) \tag{2}$$

Large differences (as much as a factor 2) exist among the different parameterizations which have been suggested for $\Phi_\varepsilon(Z/L)$; this is shown in Figure 2. In Figure 2 some of the

parameterizations were obtained directly, as mentioned above with direct measurements of the friction velocity and the dissipation rate [*Wyngaard and Coté*, 1971; *Kader*, 1992; *Fairall and Edson*, 1994]. In other studies, such as by *Large and Pond* [1981], the curve corresponds to the sum of terms 1 and 2 in (1). The large scatter in the results may explain why the parameterization of *Large and Pond* [1981, 1982], even if it neglects the imbalance term, has been frequently used. Indeed, they had shown good agreement between momentum flux estimated by eddy correlation and inertial dissipation at near-neutral conditions. However, more recent studies at more unstable stratification have shown that the imbalance term can no longer be neglected under such conditions (DWKT95; YT96). It can be noticed from Figure 2 that even for close to neutral stratification (defined here by $Z/L > -0.5$) the parameterization of $\Phi_{\text{imb}}(Z/L)$ still needs discussion.

Since the parameterization of Φ_{imb} and therefore Φ_ε is one of the major uncertainties of the inertial dissipation method, it must be established accurately for the whole range of stabilities and more particularly for unstable stratification. It is one objective of this paper to derive the parameterization that best fits the data obtained on board the R/V *Le Suroit* during the SOFIA/ASTEX and SEMAPHORE experiments. Figure 2 anticipates these results in showing the best fit for this study, obtained as described in the following sections (labeled SOFIA & SEMAPHORE). We shall describe the methodology to obtain a parameterization of Φ_ε with data not corrected for the motion of the sensors. By comparison with a parameterization of Φ_ε at neutral stratification it is possible to quantify the imbalance term by conditional sampling of the data depending on their stability, as will be described in detail below. However, we would like first to discuss another problem related to this method, i.e., its convergence.

3.2. Convergence of the Inertial Dissipation Method

The parameterizations shown in Figure 2 are not sufficient to directly provide a friction velocity because Z/L also depends on u^*, which is the unknown! *Large and Pond* [1982] suggest a method of calculating L based only on averages of the wind speed, the specific humidity, and the air-sea temperature difference using bulk parameterizations of the friction velocity and the buoyancy flux. This avoids an iterative process. However, this simplification can only apply in near-neutral stratification for which, as shown in Figure 2, Φ_ε does not strongly depend on Z/L. It is clear from Figure 2 that for $Z/L < -0.5$ this is no longer valid. Moreover, very unstable stratifications are mostly obtained at low wind speeds (<4 m/s) for which the exchange and drag coefficients are defined with great uncertainty. Bulk estimates of Z/L in order to obtain u^* by the inertial dissipation are questionable in these cases. Since such conditions were encountered during SOFIA and SEMAPHORE, we have applied an iterative process using either a bulk estimate of the buoyancy flux or a combined inertial dissipation method applied both to the wind speed and to the "virtual" air temperature deduced from the speed of sound measured by the sonic anemometer.

In previous studies the convergence of the inertial dissipation method was generally not considered [*Fairall and Edson*, 1994; YT96]. However, we shall see below that the application of the iterative process to SOFIA/ASTEX and SEMAPHORE data gives further evidence for the necessity of including an imbalance term in the TKE budget. Indeed, this convergence process will be shown to have an impact on the flux estimates, on their parameterization, and also on the correction by the imbalance term on the inertial dissipation method.

The solution of the inertial dissipation method has to solve the system of equation (1) or (2) and

$$L = \frac{-T_v u^{*3}}{g\kappa\langle wt_v\rangle} \tag{3}$$

One usual way to solve this system is to iterate from neutral conditions with $Z/L = 0$ and continue until a convergence threshold is reached on u^*. Let us remark here that this can be applied only in the case of a monotonically decreasing function Φ_ε. In the case of functions of the forms proposed by *Fairall and Edson* [1994] and YT96, the iteration must start from an initial value of Z/L that has to correspond to the local minimum of Φ_ε. Taking that into account, the procedure we use to derive the friction velocity from the inertial dissipation technique is to reinject u^* in the calculation of the Monin-Obukhov length until a criterion of convergence is reached (here we have chosen a variation of u^* of less than 0.5%).

In fact, we use two different algorithms. The first one corresponds to a more common procedure in which the buoyancy flux, $\langle wt_v\rangle$, is determined by a bulk parameterization and therefore uses the averaged values of air temperature (T), specific humidity (Q), and SST. Since this first algorithm used bulk parameterizations for the buoyancy flux, we shall denote it the dissipation-bulk (DB) algorithm in the following. Another way of performing the iterations is to involve at each step the dissipation rates for both wind and virtual temperature energy. This second algorithm will be mentioned as the dissipation-dissipation (DD) algorithm. Indeed, the use of the sonic anemometer can be optimized by exploiting both wind speed and speed of sound fluctuations. In a similar manner to the stress, the inertial dissipation method for heat fluxes is based on the budgets of scalar variance [*Large and Pond*, 1982]. Under stationary, horizontally homogeneous conditions it simplifies to

$$\langle wt\rangle \frac{\partial T}{\partial z} + \frac{1}{2}\frac{\partial\langle wt^2\rangle}{\partial z} + N_t = 0 \tag{4}$$

$$\langle wq\rangle \frac{\partial Q}{\partial z} + \frac{1}{2}\frac{\partial\langle wq^2\rangle}{\partial z} + N_q = 0 \tag{5}$$

which can also be applied to the virtual temperature. If the transport terms $\frac{1}{2}(\partial\langle wt^2\rangle/\partial z)$ and $\frac{1}{2}(\partial\langle wq^2\rangle/\partial z)$ are neglected, for the buoyancy flux it simplifies to

$$\langle wt_v\rangle_{\text{DISS}} = [\kappa Z u^* N_{tv}/\Phi_{tv}(Z/L)]^{1/2} \tag{6}$$

where in (4), (5), and (6), N_t, N_{tv}, and N_q are the turbulent dissipation rates for temperature, virtual temperature, and humidity variance and Φ_t, Φ_{tv}, and Φ_q are the universal stratification functions. These functions are assumed to be similar for the three passive parameters. Pseudo buoyancy fluxes can be derived from the sonic anemometer since the temperature provided by this device is very close (to better than 0.20%) to the virtual temperature and the magnitude of the fluxes are closely related

$$T_{\text{sonic}} = T(1 + 0.518R) = c^2/R_a\gamma \tag{7a}$$

$$\langle wt_{\text{sonic}}\rangle = \langle wt\rangle(1 + 0.518R) + 0.518T\langle wr\rangle \tag{7b}$$

$$\langle wt_v\rangle = \langle wt\rangle(1 + 0.62R) + 0.62T\langle wr\rangle \tag{7c}$$

where R is the mixing ratio and R_a and γ are the universal gas constant and the specific heat ratio ($R_a\gamma$ is 403 $m^2 s^{-2} K^{-1}$ for air). The air temperature T is expressed in kelvins. For unstable stratifications with a Bowen ratio of about 0.2, as was mainly observed during SOFIA and SEMAPHORE, this approximation leads to an underestimation of the buoyancy flux of about 4%. We have considered that this error to be acceptable, but for other conditions it would be easy to avoid this assumption if another independent heat flux was available or if assumptions concerning the transfer coefficients for temperature and humidity were made. Thus, for the solution of the inertial dissipation equations the sonic temperature energy dissipation rate can be used to approximate the buoyancy flux and thus an estimate of the Monin-Obukhov length without any bulk assumption.

This second (DD) approach would seem the more elegant for the determination of turbulent fluxes by the inertial dissipation method. However, as discussed by *Kaimal and Gaynor* [1991], the inertial subrange of the virtual temperature is not always well defined because the spectra are contaminated by noise (for more discussion see DWKT95). Therefore the first bulk approach algorithm (DB) has to be used in these cases.

When these iterative processes are applied, a problem of convergence occurs in some cases. For example, *Greenhut and Khalsa* [1995], investigating the turbulent fluxes at low wind speeds in the western equatorial Pacific Ocean (presumably at unstable stratification), mentioned the problem of convergence of the inertial dissipation method. Although they did not discuss the effect of the imbalance term separately, they remarked that Φ_ε from *Wyngaard and Coté* [1971] provided a better convergence (98% of their samples) than Φ_ε of *Large and Pond* [1981] (only 50% of their samples converged). This can be easily understood from Figure 2 since the parameterization of *Wyngaard and Coté* [1971] decreases slower with Z/L (lower slope in Figure 2) than that of *Large and Pond* [1981] in the range of unstable stratification ($Z/L < -1$).

In the next sections we shall consider this problem of convergence and see if solutions of systems (2) and (3) can always be found, especially at low wind speeds or unstable stratification. By comparing the two iterative algorithms involving either a bulk parameterization (DB) or estimates by the inertial dissipation method (DD) of the buoyancy flux, we shall show that the very high rate of divergence of the calculations in certain conditions depends on the parameterization of Φ_{imb} in the TKE budget.

3.3. Parameterization of the Imbalance Term in Φ_ε

3.3.1. Need for an imbalance term. We have noted above that using a conventional inertial dissipation algorithm for SOFIA/ASTEX and SEMAPHORE data (bulk estimates of Z/L and no iterations), DWKT95 found C_{dn} values which were much lower than in other studies. Using a bulk estimate of Z/L, Figure 3 illustrates that lower C_{dn} values are obtained for the whole data set (dots), as compared to the C_{dn} values for a near-neutral subset of the data (open diamonds with the line corresponding to mean values in bins of 2 m/s). This remains true whether a varying or constant value is used for C_{hn} and C_{en} (compare Figures 3a and 3b). Thus, using a classical algorithm, a dependence of C_{dn} on the stability is evident. This discrepancy suggests that it is necessary to add the transport terms in the TKE budget to eliminate this dependence on the stability.

However, using an iterative algorithm but still neglecting the transport terms in the TKE budget, we found, like *Greenhut and Khalsa* [1995], that there is a crucial problem of divergence of the calculation. For example, Table 3 will show later that in these conditions only 30% of the SOFIA/ASTEX and SEMAPHORE data converged for wind speeds below 5.5 m/s. The corresponding Z/L are all near-neutral ($Z/L > -1$); that is, the data which did not converge were mainly unstable and corresponded to the anomalously low C_{dn} values by the noniterative process. Our conclusion is therefore the same as for the noniterative algorithm; a stratification dependent term has to be added to the TKE budget. This correction, which will be associated with an imbalance term, must result in no stability dependence and higher averaged C_{dn} values when using a noniterative algorithm or allow more data to converge when using an iterative method. Let us now describe how a quantitative form for the imbalance term can be determined.

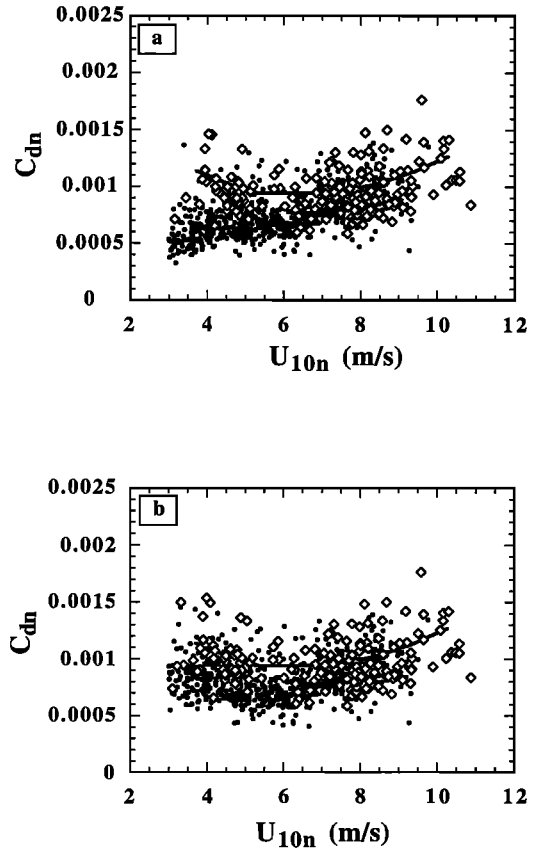

Figure 3. Drag coefficients obtained from the momentum fluxes for the whole data set from SOFIA and SEMAPHORE (dots) while neglecting transport terms in (2). The subset for near-neutral stratifications (corresponding to $0 > Z/L > -0.3$) is shown with open diamonds. The line joins means of near-neutral subset grouped in 2 m/s bins. (a) The effect of varying C_{hn} and C_{en}. (b) Constant transfer coefficients.

3.3.2. Method of determining Φ_{imb}. Since the scatter between the previously published parameterizations of Φ_ε is high and the range of stability conditions generally does not cover the "very" unstable stratifications observed during SOFIA and SEMAPHORE, we have investigated the parameterization of Φ_ε from the latter data sets. Because a direct estimate of the friction velocity was not available, the following method was used. Given that the inertial dissipation technique has been verified at near-neutral stratifications (by *Large and Pond*

[1981], for example), we can assume a formula for Φ_ε in those conditions. Thus, for $0 > Z/L > -0.3$, Φ_ε is defined with $\kappa = 0.4$ and Φ_m from *Dyer* [1974] and Φ_{imb} set to zero. This "near-neutral" data set was used to obtain friction velocities and the corresponding parameterizations of the drag coefficient as a function of the wind speed at 10 m for Z/L near zero using an iterative algorithm as described in section 3.2. In order to increase the data available and hence the statistical significance of this analysis, the buoyancy flux has been computed from a bulk formula in the derivation of L instead of using the dissipation technique (DB algorithm). One hundred and ten samples (out of 981) were found with $0 > Z/L > -0.3$, corresponding to wind speeds ranging from 3 to 11 m/s. The magnitude of the near-neutral C_{dn} thus calculated has been shown in Figure 3. These C_{dn} values have then been used to derive a "true in average" friction velocity by using a bulk parameterization. In other words, we replace the direct estimates of the friction velocity, which are necessary to derive Φ_ε, with bulk estimates. It is only true in average because a bulk estimate does not account for the variability of the C_{dn} caused in part by effects such as wave age [*Nordeng*, 1991; *Toba et al.*, 1990; *Smith et al.*, 1992] or directional properties of the wave fields [*Donelan et al.*, 1997]. We are assuming here that for a chosen combination of stability and U_{10n} the effect of the transport terms on the mean magnitude of C_{dn} is much greater than that of the dependence of the drag on other parameters. This is reasonable since these other parameters are more likely to increase the scatter rather than bias the mean. So, if we consider that this near-neutral bulk estimate of the friction velocity is equivalent to an averaged value of direct estimates of the friction velocity, the imbalance term can then be deduced from the two different estimates of u^*: from the bulk formulas (u^*_{bulk}) and from the inertial dissipation technique neglecting Φ_{imb} (u^*_{dissip})

$$u^{*3}_{\text{bulk}} = [\sqrt{C_{dn}}\, U_{10n}]^3 = \frac{\kappa Z \varepsilon}{\Phi_m(Z/L) - Z/L - \Phi_{\text{imb}}(Z/L)} \tag{8}$$

$$u^{*3}_{\text{dissip}} = \frac{\kappa Z \varepsilon}{\Phi_m(Z/L) - Z/L} \tag{9}$$

where L is the same in (8) and (9). Thus solving (8) and (9) for ϕ_{imb},

$$\Phi_{\text{imb}}(Z/L) = [\Phi_m(Z/L) - Z/L]\left[1 - \frac{u^{*3}_{\text{dissip}}}{u^{*3}_{\text{bulk}}}\right] \tag{10}$$

3.4. Choice of Exchange Coefficients, C_{en} and C_{hn}

At low wind speed the uncertainty on the exchange coefficients for heat and humidity is still high. However, the choice of low wind speed parameterization is important for very unstable stratification when the buoyancy dominates the shear. For calculation of the imbalance term, two cases have been considered: one with constant exchange coefficients of 1.2×10^{-3} and the other with exchange coefficients of constant value of 1.2×10^{-3} above 5.2 m/s, increasing as U_{10n} decreases to lower wind speeds. The form of this varying exchange coefficient was obtained from the SEMAPHORE experiment using the inertial dissipation method with the virtual temperature of the sonic. It will be discussed in detail in section 4.2. Although this varying exchange coefficient is in agreement with other recent studies, many authors still use constant C_{hn} or C_{en}, even at very low wind speeds. It was therefore of interest to compare the impact of the two parameterizations on the imbalance function; the results will be presented in section 4.3.

3.5. Consideration of the Free Convection Regime

It will be shown below that when buoyancy fluxes were determined using the dissipation technique (with the DD algorithm), Z/L values were found to vary between 0 and -8. Thus, for the most unstable stratifications (associated with low wind speeds), free convection limits should be applied. According to *Beljaars* [1995] the Monin-Obukhov similarity theory is still valid for the free convection regime, provided a term of wind gustiness, W_g, is added to the average horizontal wind speed, U. This gustiness factor is due to the transfer of energy from the vertical to the horizontal of wind components at regimes for which convection dominates, with a vertical velocity scale w^* defined as

$$w^* \equiv \left[\frac{g}{T_v}\langle wt_v\rangle H\right]^{1/3} \tag{11}$$

where H is the height of the mixed layer in the atmosphere. There are two important unknowns in this "simple" theory. The first one concerns the relationship between W_g and w^*. Experimental studies have lead to (at standard timescales and space scales for the fluxes)

$$W_g = 1.2w^* \tag{12}$$

The second uncertainty concerns the way the gustiness factor adds to the mean wind speed. *Beljaars* [1995] proposes a quadratic relationship with

$$S = \sqrt{U^2 + W_g^2} \tag{13}$$

The disadvantage of this approach is that these empirical functions depend on the timescales or space scales used in the analysis as compared to the convective cells. *Beljaars*' [1995] paper refers to large-scale models. Further studies will therefore be needed for this theory to be accurately applied to mesoscale measurements. Another term to include in order to match free convection limits concerns the stratification functions. Indeed, the replacement of u^* by w^*, as for the velocity scale in the free convection regime, implies that Φ_m takes the form

$$\Phi_m = (1 - d)(1 - aZ/L)^{-0.25} + d(1 - aZ/L)^{-0.33} \tag{14}$$

with the factor d tending towards 0 and 1 for neutral and very unstable conditions, respectively. In this paper we have used the same formulation for d as proposed by *Fairall et al.* [1996] for the TOGA-COARE bulk algorithm and *Dyer*'s [1974] constant, $a = 16$, has been used for the stability function. Because of the assumptions needed in this free convection treatment, the results will be presented below including a free convection parameterization (FC results) and a no free convection parameterization (NFC), where in general we have chosen to recommend the NFC values.

4. Results

4.1. Definition of the Flow Regimes

Two regimes defined by the roughness of the flow, with the separation between aerodynamically smooth or rough conditions have been considered. Inspection of the preliminary results suggested that a minimum occurred in the transfer coefficient values at wind speeds between 5 and 6 m/s. Regression

Table 1. Coefficients of Regressions in the Fit of the Neutral Transfer Coefficient for Temperature From the Sonic Anemometer as a Function of the Wind Speed U_{10n}

Hypotheses		$U_{10n} < 6$ m/s: $C_{hn} = a\ U_{10n}^{-1} + b$			$U_{10n} > 5$ m/s: $C_{hn} = a\ U_{10n} + b$			
α	NFC/FC	$a \times 10^3$	$b \times 10^3$	Percent of Convergence	$a \times 10^3$	$b \times 10^3$	Percent of Convergence	Mean $\times 10^3$
0	NFC	6.49	−0.01	15	0.01	1.19	97	1.23
−0.25	NFC	2.63	0.73	47	0.01	1.14	100	1.22
−0.5	NFC	2.79	0.66	72	0.02	1.09	100	1.20
−0.65	NFC	2.35	0.74	82	0.02	1.08	100	1.20
0	FC	1.33	0.77	61	0.03	0.89	100	1.13
−0.25	FC	1.84	0.72	75	0.03	0.93	100	1.15
−0.5	FC	1.16	0.91	85	0.03	0.96	100	1.16
−0.65	FC	1.23	0.90	86	0.03	0.97	100	1.16

Two different regimes are distinguished for U_{10n} greater or less than 5.5 m/s, but an overlap is used for the regressions to be consistent. Results are shown for different values of the imbalance coefficient α and for no free convection (NFC) and free convection (FC) parameterizations. In each case the percentage of data for which the iteration converged is also shown.

fits for the transfer coefficients, based on the minimization of the flux errors, will be therefore presented for $U_{10n} < 6$ m/s and for $U_{10n} > 5$ m/s (where the overlap in the ranges ensures continuity between the regimes). The calculated regressions may be considered valid below and above 5.5 m/s for the smooth and rough regimes, respectively.

4.2. Transfer Coefficients for Sensible and Latent Heat

We have noted above that using the speed of sound measurements from the sonic anemometer, it is possible to deduce a value which is an approximation (within a few percent) for the flux of virtual temperature, that is, the buoyancy flux. In order to calculate the sensible heat flux from the "sonic temperature flux" we use

$$\langle wt \rangle = \frac{\langle wt_{\text{sonic}} \rangle}{1 + 0.518\, Q_{10n} + 0.518(T_{10n})\dfrac{(Q_{\text{sat}} - Q_{10n})}{(\text{SST} - T_{10n})}} \tag{15}$$

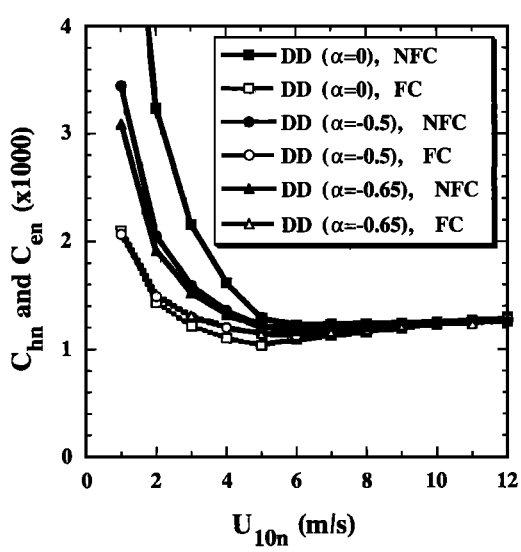

Figure 4. Regression fits for the transfer coefficients C_{hn} and C_{en}, obtained from the DD algorithm as a function of U_{10n}. Relationships are shown for the different imbalance terms ($\Phi_{\text{imb}}(Z/L) = \alpha Z/L$) with $\alpha = 0$, −0.5, and −0.65 and for no free convection (NFC) and free convection (FC) parameterizations.

This can be derived from (7b) by assuming that the transfer coefficients for temperature and humidity are equal, $C_{en} = C_{hn}$, so that $\langle wq \rangle = \langle wt \rangle[(Q_{\text{sat}} - Q_{10n})/(\text{SST} - T_{10n})]$. The resulting formulae for C_{hn} and C_{en} are summarized in Table 1 and Figure 4. Anticipating the results for the imbalance term, $\alpha Z/L$ (section 4.3), coefficients are shown for a range of α values, as well as for NFC and FC parameterizations and the smooth and rough wind regimes.

For the smooth flow regime ($U_{10n} < 5.5$ m/s) the coefficients are found to increase with decreasing wind speeds. However, the increase is less rapid than will be shown for the C_{dn} values (section 4.4), and a power law such as ($a\ U_{10n}^{-1} + b$) is found to fit the data. Concerning the C_{en} dependence on α, Figure 4 shows that it is relatively small. The main effect of increasing α is to increase the proportion of cases which converge (Table 1) especially for the NFC case. For those cases which converge, the small dependence on α is because the stratification function $\Phi_{tv}(Z/L)$ dominates over u^* in (6).

At higher wind speeds ($U_{10n} > 5.5$ m/s), because of the small number of samples the statistical significance of the linear regressions displayed in Table 1 is poor. As C_{hn} or C_{en} values are usually found to be constant, the mean values for the rough flow regime are also given in Table 1. Hence the parameterization derived from the SEMAPHORE data using the sonic anemometer leads to

$$C_{en} \times 10^3 = C_{hn} \times 10^3 = 2.79 U_{10n}^{-1} + 0.66 \qquad U_{10n} < 5.2 \text{ m/s} \tag{16a}$$

$$C_{en} \times 10^3 = C_{hn} \times 10^3 = 1.2 \qquad U_{10n} > 5.2 \text{ m/s} \tag{16b}$$

where the proposed threshold has been modified to 5.2 m/s to allow continuity of the transfer coefficient values across the threshold. Equations (16a) and (16b) were the ones used for the DB algorithm for the case of varying exchange coefficients.

The variation of the roughness length for humidity, z_q, values for $U_{10n} > 3$ m/s have been discussed in a previous paper (DWKT95) where latent heat fluxes from a Lyman-α hygrometer were also used. This analysis also showed a statistical decrease of z_q with U_{10n} in contrast with the dynamic roughness z_0.

4.3. Imbalance Term

The effect of the free convection assumptions in the determination of the imbalance function in the TKE budget is

Table 2. Coefficients of Regression and Correlation in the Linear Regression Between ϕ_{imb} and Z/L for Different Hypotheses

Hypotheses		ϕ_{imb} (Z/L)	
NFC/FC	C_{hn} or C_{en}	Equation of Regression	Coefficient of Correlation
NFC	1.2×10^{-3}	$-0.31Z/L - 0.021$	−0.41
NFC	varying	$-0.69Z/L - 0.166$	−0.90
FC	1.2×10^{-3}	$-0.27Z/L - 0.044$	−0.37
FC	varying	$-0.65Z/L - 0.136$	−0.88

Constant or varying C_{hn} and C_{en}.

shown in Table 2 together with the results for the two different formulations for the transfer coefficients, C_{hn} and C_{en}. The coefficient α for the imbalance terms is found to vary between −0.69 and −0.27, the effect of the choice in C_{hn} $(= C_{en})$ being much more significant than whether the free convection is parameterized or not.

The dependence on C_{hn} and C_{en} is explained by Figure 5, which shows the imbalance terms deduced from (10), Φ_{imb}, as a function of Z/L for all data of SOFIA and SEMAPHORE with $3 < U_{10n} < 11$ m/s. The effect of allowing C_{en} and C_{hn} to increase at low wind speed (as in (16a)) is to increase the calculated buoyancy flux at wind speeds <5 m/s (Figure 5a), resulting in significantly more unstable values of Z/L compared to using constant transfer coefficients (Figure 5b). Inspection of Figure 5 shows that a linear regression fitted to the data for Z/L values corresponding to near-to-neutral stability tends to give a smaller slope than is obtained for a greater range of Z/L. Therefore we shall introduce the regression coefficient α to define the imbalance term in the inertial dissipation, with

$$\Phi_{imb}(Z/L) = \alpha Z/L \tag{17}$$

Thus the linear fits for the imbalance term are obtained with α equal to −0.69 and −0.31 (with a correlation coefficient of −0.9 and −0.4) for the varying and constant exchange coefficients, respectively. The low correlation in the second case is caused by the smaller range of Z/L.

The first parameterization, with a higher level of confidence and C_{hn} and C_{en} values derived (section 4.2) from the DD algorithm, was included in the Φ_ε function of Figure 2 labeled SOFIA & SEMAPHORE. For unstable stratifications ($Z/L < -1$) this new parameterization of Φ_ε is found to converge in more cases than the other parameterizations and to compare better with *Kader* [1992] or *Wyngaard and Coté* [1971] than with *Large and Pond* [1981]. For the remainder of this paper we will consider the correction to be $\Phi_{imb} = -0.65Z/L$, as obtained with the DB algorithm, with varying C_{en} and C_{hn}. As compared to some previous studies, this value is somewhat larger in magnitude. For example, *Lenschow et al.* [1980] found a coefficient of −0.4 from aircraft measurements. Although most studies found a linear law between the transport terms and Z/L, some authors have proposed other forms. For example, *Frenzen and Vogel* [1992] have proposed $\Phi_{imb} = 0.1Z/L + [1/(7 - Z/L)]$.

Using a very similar approach to this paper, based on shipboard estimates by the inertial dissipation method, YT96 proposed an imbalance term which depended on the wind speed. Their value for $\alpha(= 2 - (U_{10n}/3))$ agrees with that proposed here for winds of about 8 m/s. At higher wind speeds, α becomes increasingly negative, but because the typical magnitude of Z/L decreases, YT96's average imbalance term tends to remain approximately constant with increasing winds. For these higher wind speeds, which included most of the YT96 data, the success of the imbalance term in removing the stability dependence of the u^* values gave confidence in the formula that they proposed. However, at wind speeds below 6 m/s the α suggested by YT96 becomes positive. That implies that the C_{dn} values for unstable stratification found in SOFIA and SEMAPHORE, which are already too low, would be decreased even further compared to the neutral value. It is surprising then that the C_{dn} to U_{10n} relationship proposed by YT96 will be shown below to agree with our results. YT96 had few data in this region, and it may be that the imbalance term that they proposed had the effect of removing the nonneutral values (through nonconvergence of the iteration). Only the near-neutral data would then have remained for which the imbalance was negligible. A similar argument is offered below for the apparently small effect on C_{dn} of the formulation for the imbalance term at low wind speeds (section 4.4.2).

4.4. Drag Coefficient

4.4.1. Comparison of dissipation-dissipation (DD) and dissipation-bulk (DB) algorithms. In the previous sections we have calculated values for the transfer coefficients C_{hn} and

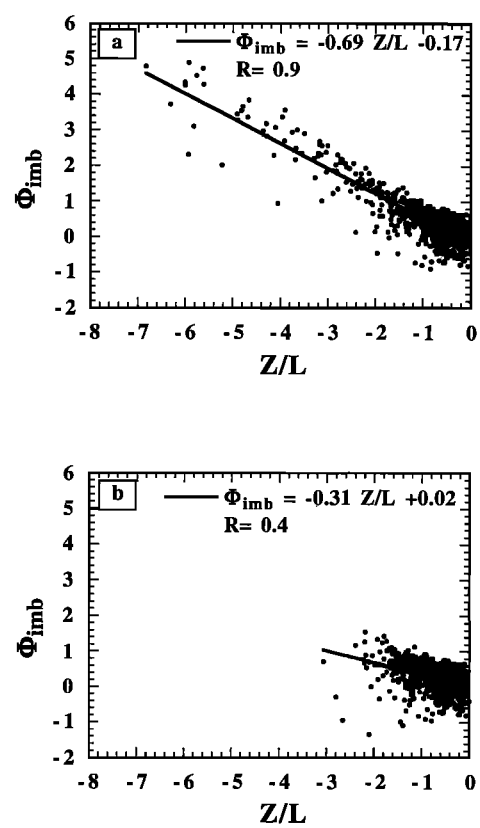

Figure 5. Scatter diagrams of the turbulent transport term Φ_{imb}, obtained from (10) as a function of Z/L for all data from SOFIA and SEMAPHORE with $3 < U_{10n} < 11$ m/s. For these calculations the DB algorithm is used to increase the number of samples. However, this algorithm implies assumptions for the transfer coefficients C_{hn} and C_{en}. (a) C_{hn} and C_{en} vary with wind speed (see text). (b) $C_{hn} = C_{en} = 1.2 \times 10^{-3}$.

Table 3. Coefficients of Regressions in the Fit of the Neutral Drag Coefficient C_{dn} From the Longitudinal Wind Component Measured by the Sonic Anemometer as a Function of the Wind Speed U_{10n}

Hypotheses			$U_{10n} < 6$ m/s: $C_{dn} = a\ U_{10n}^{-2} + b$			$U_{10n} > 5$ m/s: $C_{dn} = a\ U_{10n} + b$		
α	NFC/FC	DB/DD	$a \times 10^3$	$b \times 10^3$	Percent convergence	$a \times 10^3$	$b \times 10^3$	Percent convergence
0	NFC	DD	8.51	0.60	15	0.044	0.66	97
−0.25	NFC	DD	5.71	0.80	47	0.016	1.01	100
−0.5	NFC	DD	10.20	0.91	72	−0.011	1.34	100
−0.65	NFC	DD	11.39	1.05	82	−0.025	1.52	100
0	FC	DD	5.26	0.70	61	0.030	0.81	100
−0.25	FC	DD	7.92	0.85	75	0.007	1.12	100
−0.5	FC	DD	10.18	1.02	85	−0.015	1.39	100
−0.65	FC	DD	12.33	1.07	86	−0.027	1.55	100
0	NFC	DB	12.53	0.43	31	0.044	0.60	70
−0.25	NFC	DB	11.20	0.48	56	0.045	0.64	85
−0.5	NFC	DB	10.85	0.59	81	0.031	0.84	92
−0.65	NFC	DB	11.70	0.67	86	0.020	0.98	91
0	FC	DB	12.52	0.46	32	0.043	0.61	72
−0.25	FC	DB	11.76	0.48	58	0.041	0.68	87
−0.5	FC	DB	11.43	0.60	82	0.027	0.88	92
−0.65	FC	DB	12.10	0.68	87	0.017	1.01	91

Two different regimes have been distinguished with an overlap in the U_{10n} ranges, as in Table 1, for the regressions to be consistent. Results are shown for different values of the imbalance coefficient α for no free convection (NFC) and free convection (FC) parameterizations, and for DB and DD algorithms. In each case the percentage of data for which the iteration converged is shown.

C_{en} using the DD algorithm. Then we used these values in a DB algorithm to establish the imbalance term. Use of the DB algorithm provides around 1000 samples from SOFIA plus SEMAPHORE, whereas for the DD algorithm, only about 80 samples are available from SEMAPHORE. For both algorithms, results for C_{dn} are shown in Table 3 for different values of the imbalance term, for NFC and FC parameterizations, and for both flow regimes. Comparison of the results for DD and DB algorithms suggests that the differences are significant. However, this is misleading since different proportions of data converged and since the DD results were limited to a small subset of the SEMAPHORE data; indeed, it will be shown later that a systematic difference existed in the results from the two experiments.

Figure 6 compares u^* values for all samples where results from both DD and DB algorithms were available. The reference is taken to be u^* values by the DB algorithm with the imbalance function of $-0.65Z/L$. This reference is compared in Figures 6a–6d with four different imbalance functions used in the DD algorithm. The agreement between the two algorithms would correspond to α set halfway between −0.50 and −0.65 for the DD algorithm. In the following, we shall use the DD algorithm with $\alpha = -0.50$; although both algorithms also correspond well with $\alpha = -0.65$, the determination of the optimal value for α should be done with a larger data set. This small discrepancy between the two algorithms might be related to the transport term in the budget of variance of virtual temperature for deriving the buoyancy flux. Indeed, the calculation of the buoyancy flux by (6) does not include the transport term for which parameterizations have been proposed, for example, by *Kaimal et al.* [1976]. Resolving this new question is beyond the scope of the present paper.

4.4.2. Effect of the imbalance term on convergence. Table 3 shows that the rate of convergence is much smaller for the smooth regime than for the rough regime, respectively characterized by unstable and near-neutral stratification. One major effect of the imbalance term is to increase the convergence rate; for example, it increases from 30% ($\alpha = 0$) to near 90% ($\alpha = -0.65$) for the smooth regime using the DB algorithm. As a result, the apparent effect of the imbalance term on C_{dn} can be characterized in terms of three domains defined by high, midrange, and low wind speeds and dominated by neutral, slightly, and strongly unstable stratifications, respectively.

Considering first the dissipation-bulk algorithm (Table 3 and Figure 7a), at low wind speeds and with no imbalance term, only the near-neutral cases converge. An imbalance term of −0.25 results in more cases converging, and mean C_{dn} values slightly lower than the neutral value are calculated. For $\alpha = -0.5$ and −0.65 even more cases converge, and since this appears to be the correct magnitude for the imbalance term, the calculated C_{dn} values are again similar to the neutral cases. Thus, for these very low wind speeds the C_{dn} values are forced to agree with the near-neutral values (because other cases do not converge), and the calculated C_{dn} is apparently independent of the imbalance term. Probably for the same reason, the results are similar for both NFC and FC parameterizations. At moderate wind speeds many more cases converge irrespective of the choice of the imbalance term. Without an imbalance term the calculated C_{dn} values are much lower than the neutral value, and it is in this wind speed range that the correct choice of the imbalance term is vital. At higher wind speeds the stability is closer to neutral, and the calculated C_{dn} values therefore lie nearer to the correct neutral value regardless of the choice of α.

Considering now the DD algorithm (Table 3 and Figure 7b), there is a significant difference in the rate of convergence depending on whether the free convection parameterization is included (FC) or not (NFC). For this algorithm the formulation for the imbalance term has much more effect. When u^* increases, the buoyancy flux is forced to decrease (caused by term Φ_{tv} in (6)), forcing an inverse variation of C_{en} (and C_{hn}) compared to C_{dn}. In comparison, in the DB algorithm the buoyancy flux is only affected by the change in Z/L. Near-neutral values of C_{dn} are achieved with a smaller magnitude for the imbalance term, $-0.5Z/L$ for the NFC case and even less for the FC case. However, as was noted above (section

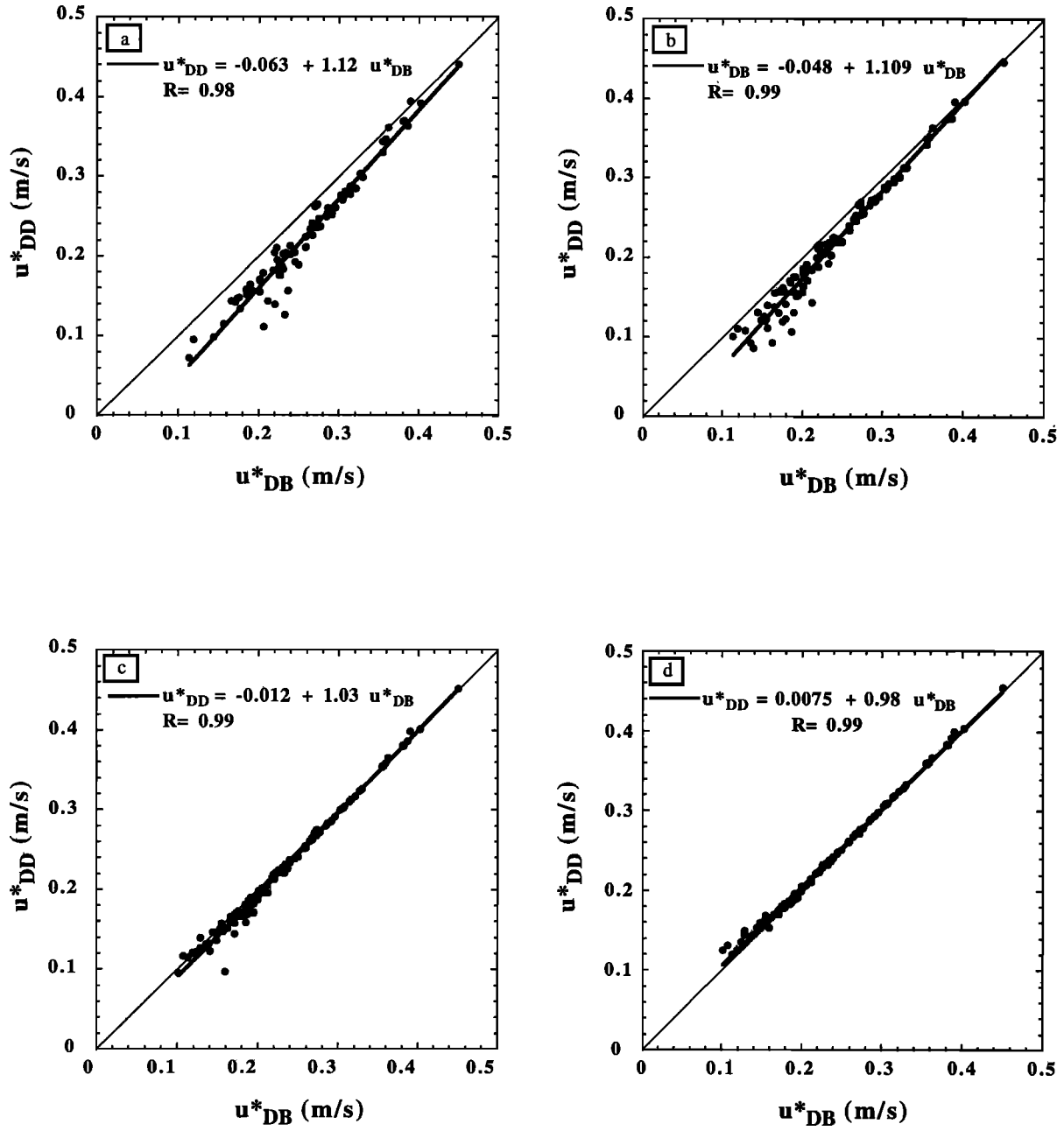

Figure 6. Comparison of the two algorithms for the inertial dissipation method (DD and DB). The reference is taken as u^* from the dissipation bulk (DB) algorithm, with the imbalance function of $-0.65Z/L$ as found in Figure 5. The reference is compared with the u^* from DD algorithm for different imbalance functions: (a) $\alpha = 0$, (b) $\alpha = -0.25$, (c) $\alpha = -0.5$, and (d) $\alpha = -0.65$.

4.4.1), the much smaller data set available for this algorithm hinders direct comparison with the average DB results.

4.4.3. Drag coefficient for the smooth flow regime. We shall consider first the drag coefficients obtained for $U_{10n} <$ 5.5 m/s. Irrespective of the choice of imbalance function or algorithm a very strong increase of the drag coefficients was found for decreasing wind speeds for data from both SOFIA and SEMAPHORE. The C_{dn} values at 0.5 m/s were of order 10–100 times higher than what was found at 5.5 m/s. This increase is in agreement with other recent studies at low wind speeds. Indeed, observations by *Greenhut and Khalsa* [1995] and YT96 are in agreement with C_{dn} values for low wind speeds. For example, Figure 8 gives C_{dn} values for the cases $\Phi_{\text{imb}} = -0.5Z/L$, (DD, NFC), and $\Phi_{\text{imb}} = -0.65Z/L$, (DB, NFC), compared to fits obtained in other studies. In contrast, the equation proposed by *Cardone* [1969], $z_0 = 0.684\, u^{*-1} + 4.28 \times 10^{-5}\, u^{*2} - 0.0443$, converted to C_{dn} leads to much smaller values. This parameterization by Cardone is actually used in several operational models. It shows how significant the uncertainties on flux parameterization in low wind conditions remain. From the SOFIA and SEMAPHORE data set the best fit for C_{dn} at low wind speeds is

$$C_{dn} \times 10^3 = 11.7000 U_{10n}^{-2} + 0.6680 \qquad U_{10n} < 5.5 \text{ m/s} \qquad (18)$$

Figure 9 shows the friction velocity as a function of U_{10n} with the data for SOFIA and SEMAPHORE averaged separately in 1 m/s wind speed ranges. For both DD and DB algorithms for SEMAPHORE and for the DB algorithm for SOFIA the low wind speed results show an asymptotic value of $u^* = 0.1$ m/s as the wind speed tends toward 0 m/s. Thus, at wind speeds below 3 m/s, u^* is no longer dependent on U_{10n}; this range is associated with the free convection regime.

4.4.4. Drag coefficient for the rough flow regime. Concerning the aerodynamically rough regime of C_{dn} values ($U_{10n} > 5.5$ m/s), the upper range of wind speeds in this data set ($U_{10n} > 7$ m/s) are mostly corresponding to near-neutral stratifications and are little affected by the choice of hypothesis (imbalance term or free convection). Also, the iterative process converges in almost all cases (Table 3). However, since the C_{dn} values at wind speeds between 5.5 and 7 m/s are rather sensitive to the choice of imbalance term and the amount of higher wind speed data is small, we shall not attempt to define a quantitative relationship for the dependence of C_{dn} on U_{10n} for the rough regime using these data. Figure 8 suggests that

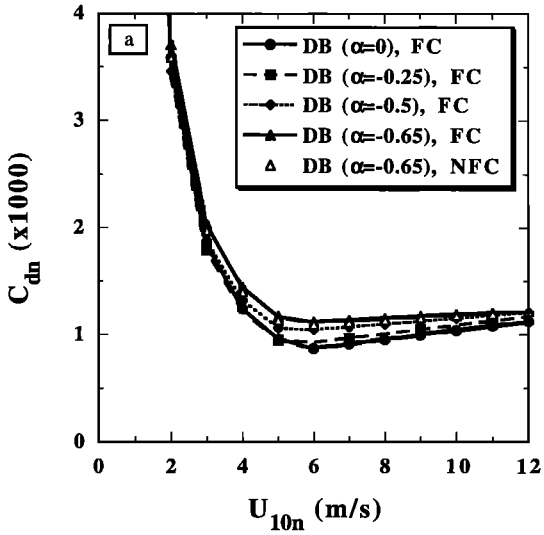

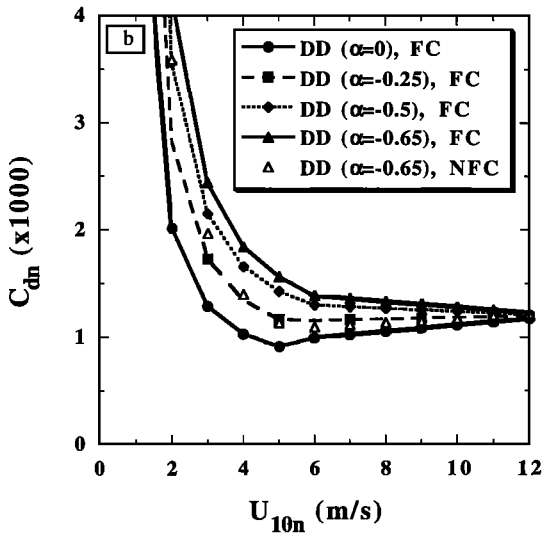

Figure 7. Regression fits for the drag coefficient C_{dn} as a function of U_{10n}. Relationships are shown for the different imbalance terms ($\Phi_{\text{imb}}(Z/L) = \alpha Z/L$) with $\alpha = 0$, -0.25, -0.5, and -0.65. (a) Results from the DB algorithm with the free convection (FC) parameterization included. (b) Same as Figure 7a, but for the DD algorithm. The results for the DB algorithm with no free convection (NFC) parameterization and $\alpha = -0.65$ are also shown for comparison in Figures 7a and 7b.

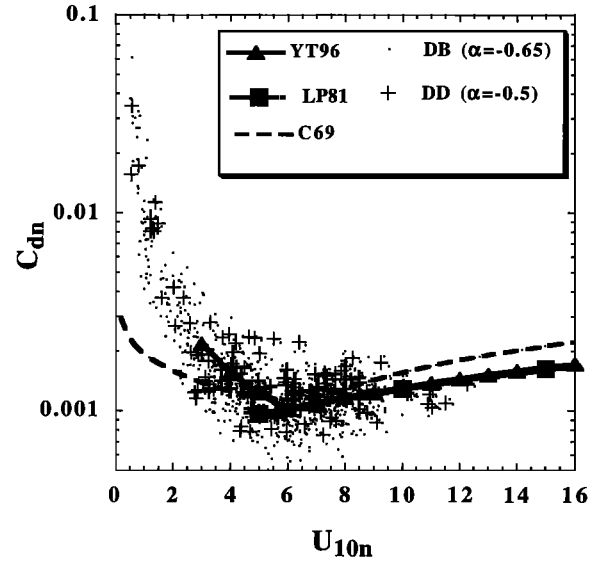

Figure 8. Comparison of the drag coefficient variations with U_{10n} for the DB algorithm with $\Phi_{\text{imb}} = -0.65Z/L$ (dots) and for the DD algorithm with $\Phi_{\text{imb}} = -0.50Z/L$ (pluses). The no free convection hypotheses (NFC) were used. Also shown are results from other studies: *Large and Pond* [1981], YT96, and *Cardone* [1969].

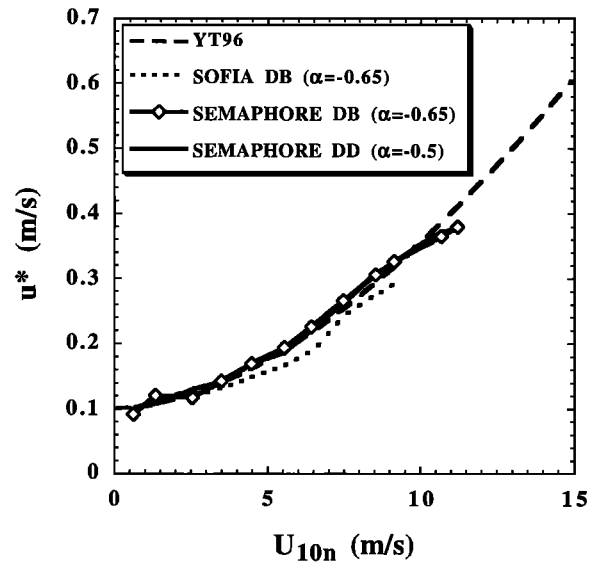

Figure 9. Friction velocities as a function of neutral wind speeds at 10 m averaged into 1 m/s wind speed ranges. Separate results are shown for SEMAPHORE and SOFIA. For SEMAPHORE, two estimates of u^* are compared: the DB algorithm, NFC, with $\alpha = -0.65$ and DD algorithm, NFC, with $\alpha = -0.50$. In most of the bins the standard error is <0.01. The results of YT96 are also shown.

the observed C_{dn} values in this wind speed range are in agreement with other studies, not all shown in Figure 8 (for example, we find an agreement within a few percent with the parameterization of *Smith* [1988]).

Considering the friction velocity as a function of U_{10n} (Figure 9) for both DD and DB algorithms, the SEMAPHORE results were in good agreement with YT96. More recent work by M. J. Yelland and P. K. Taylor (unpublished data, 1997) has used a three-dimensional computational fluid dynamic (CFD) model to correct the friction velocity estimates for air flow disturbance associated with the presence of the ship's hull and superstructure. These results suggest that the u^* values should be decreased by about 3–4% but that this reduction should be similar for both the YT96 and the SOFIA and SEMAPHORE data sets. Why the SOFIA estimates are lower than for SEMAPHORE or YT96 (Figure 9) is not explained. Thus, although we obtained consistent stress estimates from two diverse ocean regions, some uncertainties still remain.

4.4.5. Effect of the free convection parameterization. Inspection of Table 3 shows that the inclusion of a free convection parameterization does not have a great effect on the C_{dn} values, even at very low wind speeds. The main purpose of including these free convection assumptions in this study was to be able to compare the parameterizations of turbulent fluxes with other studies which have already included these assumptions. However, the effect on fluxes themselves is negligible. In the DD algorithm the impact of the free convection hypotheses on the flux estimates is restricted to the effect on the stratification functions. The gustiness factor has an effect on U_{10n} and therefore on C_{dn}, C_{en}, and their regression toward U_{10n} but has no effect at all on u^* and $\langle wt \rangle$. In contrast, in the DB algorithm a change in U_{10n} has a small impact on $\langle wt \rangle$ by the aerodynamic bulk estimates and thus on Z/L and u^*. Because of the quadratic relationship used to add the gustiness factor, the U_{10n} values are not significantly changed. Further investigations of this problem using experimental data would be interesting, for example, to relate the gustiness factor to the energy of horizontal wind spectra in the frequency range corresponding to the convection.

However, Figure 9 does give some evidence for a free convection regime. For u^* an asymptotic value of 0.1 m/s is found at zero wind speed. That a nonzero minimum friction velocity should exist under free convection conditions was suggested by *Businger* [1973] and discussed by *Schumann* [1988]. This constant value can be explained by the approach to free convection limits where u^* is no longer a relevant scale. The magnitude of the minimum friction velocity found here is the same as that obtained by *Greenhut and Khalsa* [1995]. A similar value was also indicated by the data of YT96, although those authors questioned the validity of their estimates at very low wind speeds, and the effects of instrument noise and other factors cannot be totally discounted. However, the experimental results are not inconsistent with *Beljaars'* [1995] theoretical approach for the free convection limit. The inclusion of a term S due to the gustiness factor (see (13)) in the mean wind speed will allow bulk fluxes to tend to nonzero values at zero wind speed.

5. Discussion of the Application of Turbulent Fluxes for the Free Convection Regime

Several factors suggest that we should consider in more detail the validity of the hypotheses underlying the inertial dissipation method in free convection regime conditions. In particular, there is the nonzero value of u^* (0.1 m/s) found for zero wind speed. Also, as described previously, the inertial dissipation method is based on the indirect estimates of dissipation rate of the downwind energy in the inertial subrange. The direction of stress is still, even for very low wind speeds, assumed to be aligned with the mean wind direction. However, the gustiness factor indicates that both the magnitude and the direction of the stress may vary with the spatial scale.

In discussing the inertial dissipation method (section 3), we emphasized both the iterative process and the parameterization of the transport terms in the TKE budget. While there is still an uncertainty concerning the transport terms, this uncertainty has only a small effect on the turbulent flux parameterization at low wind speeds, at least for the tendency. However, in the present section we shall consider whether other hypotheses underlying the inertial dissipation method also hold. At low wind speeds the experimental problems are increased (for example, by thermal plumes from the ship structure in the absence of natural ventilation by the wind). Also, theoretical problems appear, such as the free convection limit of the Monin-Obukhov similarity theory (discussed in section 3.5) or the validity of the Taylor hypothesis and the assumption of local isotropy.

Previous theoretical and experimental investigations of the frequency and wave number spectra of wind, temperature, or humidity fluctuations in the free convection limits have led to the following conclusions.

1. The power laws of the spectra in the inertial subrange are mainly found to follow a $-5/3$ power, both in frequency and wave number [*Kader*, 1988; *Gratchev*, 1994] (although *Gurvich and Yurchenko* [1980] have proposed a -2 power from dimensional analysis and other authors do not observe any scaling [*Foster and Waller*, 1985; *Boubnov and Golitsyn*, 1990]).

2. A $-5/3$ power law of the f or k spectra, with a dominance of three-dimensional turbulence with a cascade of energy from larger to smaller eddies, suggests that the assumption of local isotropy is valid. This implies that for the smaller eddies (that is, in the inertial subrange) the turbulence is not affected by the mean directional properties of the flow at larger scales.

3. Formulae (2) and (6) for the budget of TKE and variance of virtual temperature are also valid for free convection with practically the same empirical coefficients [*Gratchev*, 1994]. In free convection regimes, formulae for the derivation of the dissipation rates from frequency spectra become questionable since the Taylor hypothesis is no longer valid in absence of a mean flow.

We will first consider whether the wind speeds relative to the ship during light wind episodes were steady enough in magnitude and direction to be able to transform frequency to wave number through the Taylor hypothesis of frozen turbulence. To that end the standard deviations in the inertial subrange (a frequency band of 0.5–10 Hz has been chosen) have been plotted as a function of the relative wind speed in Figure 10. The line showing $\sigma_u/U_r = 0.1$ can be considered as a criterion to delimit the domain of applicability of the Taylor hypothesis ($\sigma_u/U_r < 0.1$). Figure 10 demonstrates that because of the ship speed the Taylor hypothesis can almost always be applied during SOFIA/ASTEX and SEMAPHORE. The only exceptions are a few points very near to the criterion.

A further consequence of the fact that the ship speed was at least 1–2 m/s was that the spectra were not contaminated by

the thermal plumes developing from the ship structure becaues of the lack of natural ventilation. The power laws for the frequency spectra in the inertial subrange have been examined and were found to be the same in the lower wind conditions as in the higher winds.

The last point we have checked concerns the local isotropy hypothesis not only for low wind speeds but also for the whole range of the experiments. The average of power spectral densities multiplied by the frequencies at the power 5/3 in a frequency band within the inertial subrange, $\langle E(f)\ f^{5/3}\rangle$, are shown in Figures 11a for the whole wind range and 11b and 11c for the light winds only. As mentioned in section 2, the frequency band is mainly 2–4 Hz. The downwind component is compared to the crosswind component in Figures 11a and 11b and to the vertical component in Figure 11c. The three graphs display the predicted 4/3 regression coefficient with very low scatter and generalize the conclusion that could be obtained from the single example of Figure 1 (where $E_w(f)$ was greater than $E_u(f)$ over a large frequency band covering 1–10 Hz) in the case of a low wind speed of about 1 m/s. Thus the present results confirm the local isotropy hypothesis (the predicted 4/3 downwind to lateral spectral ratio is verified) both for low winds and for the higher winds encountered and so, unlike *Wucknitz* [1979], we find that anisotropy is not to be a problem. It is evident from these successful validations of basic assumptions associated with the inertial dissipation method that a moving ship provides a better strategy for sampling in low winds than an Eulerian reference frame.

We end this discussion with an evaluation of the error due to the lack of measurements of sea surface currents in the vicinity of the ship (as described in section 2, the GPS ship velocity is relative to the seabed). The effect of surface current is proportionally much higher when the sea surface velocity magnitude is of the order of the mean atmospheric flow; that is, it should mainly affect light winds. From a statistical point of view the effect should be negligible on average for the whole data set. During the experiment, drifting buoys showed that the Azores area is dominated by geostrophic structures, spatially localized in a 50 km band and related to the Azores current. These current structures are not primarily driven by local winds and there should not be any correlation between the current and the wind measured along the ship tracks. Moreover, the research vessel performed several traverses of the Azores current while maintaining, as far as possible, a heading into the prevailing north winds. In these cases the wind and the surface current would be approximately perpendicular negating any effect of the surface currents. Concerning the smaller-scale structures of the current, inertial periods of the current would induce a modulation of the local current which would be totally decoupled from the wind speed. Because of the lack of coincident measurements on the research vessel of wind components and local sea surface current, we have decided not to allow for the current. The above arguments suggest that use of a geostrophic current would introduce more errors than enhancements.

6. Conclusion

This study of turbulent fluxes of heat and momentum by the inertial dissipation method during SOFIA/ASTEX and SEMAPHORE experiments showed that this method still requires care in its application if it is to be used in all conditions. For these data obtained over near-neutral to very unstable stratifications (for wind speeds down to a few centimeters per second and sea-air temperature differences up to 5°C), in order to reduce the dependence of the C_{dn} values on the stratification in the surface layer (Z/L), a correction factor has been shown to be necessary in the TKE budget. This term, of the order of $-0.65Z/L$, is believed to be associated with the transport terms (the sum of pressure correlation and turbulent transport in (1)), which were neglected in some other studies [*Large and Pond*, 1981; *Fairall and Edson*, 1994]. That is, it represents the imbalance between local production and dissipation of TKE; hence we have referred to it as the "imbalance term." Introduction of the imbalance term has the effect of increasing the C_{dn} values to values comparable with other studies. In other studies by ship (YT96) or by aircraft [*Lenschow*, 1974], different imbalance functions have been proposed. Thus further studies will be necessary to understand and accurately parameterize these transport terms.

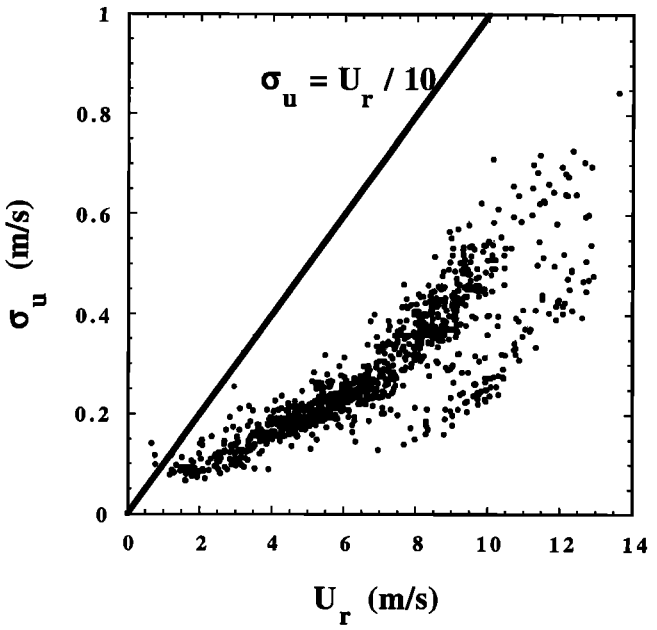

Figure 10. Scatter diagram of the wind speed relative to the ship as a function of the standard deviation of the downwind wind component in the inertial subrange (0.5–10 Hz). The line shows the limit below which the Taylor hypothesis is supposed to be valid.

Another aspect was found to be fundamental in this study: the iterative process of the inertial dissipation method. Indeed, at unstable stratifications the TKE budget is highly dependent on Z/L, and if the calculated momentum flux is not to be influenced by the initial guess of Z/L, a careful iterative process has to be used. Moreover, if only the dissipation rate of the wind energy is estimated, the problem is underdetermined and a bulk estimate of the buoyancy flux is needed with additional assumptions on the transfer coefficients for heat and humidity. These assumptions will also have an impact on the momentum flux and C_{dn} values. For that reason this study includes flux estimates by the DD algorithm, in which the sonic anemometer is used to provided both dissipation rates of thermal and wind energy. However, this technique did not lead to total agreement with the DB algorithm when the imbalance term was applied. Better agreement for the two algorithms was found for an imbalance function of $-0.65Z/L$ and $-0.50Z/L$ for the

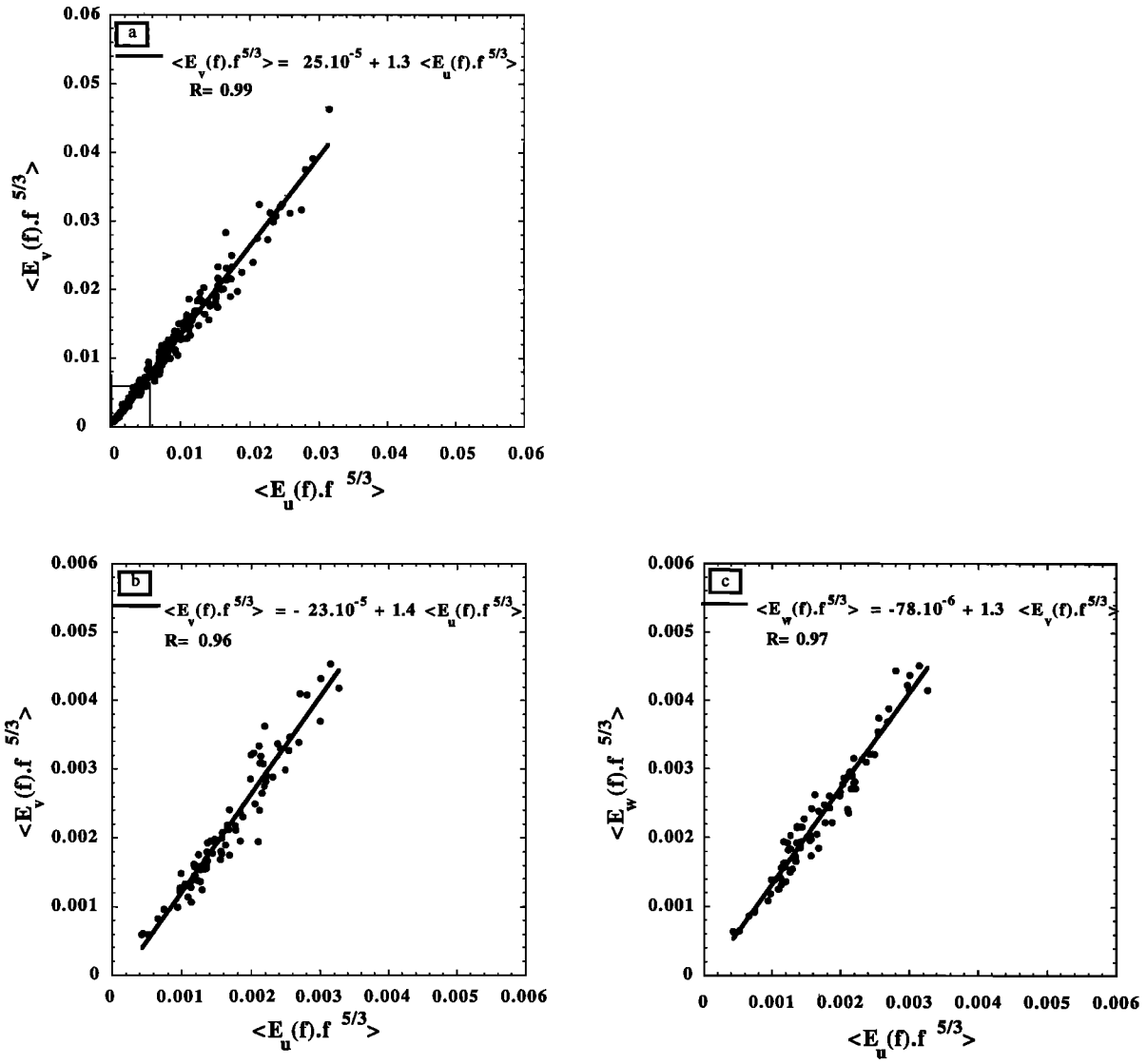

Figure 11. Scatter diagrams showing the average of spectral densities multiplied by the frequency to the 5/3 power ($\langle E(f)f^{5/3}\rangle$) in part of the inertial subrange (2–4 Hz). (a) $\langle E_u(f)f^{5/3}\rangle$ for the downwind component as a function of $\langle E_v(f)f^{5/3}\rangle$ for the cross-wind component. (b) Same as Figure 11a, but for low wind speed conditions. (c) Low wind speed conditions. $\langle E_u(f)f^{5/3}\rangle$ is also plotted as a function of $\langle E_w(f)f^{5/3}\rangle$ for the vertical wind component. For Figures 7a–7c the slope is very close to 4/3, even at the lower bounds of the wind speed.

DB and DD algorithms, respectively. This difference might be related to the transport term in the equation of the budget of temperature and humidity variance. Again, more validation of the DB method is needed, particularly with regard to determination of the heat fluxes.

Despite the remaining uncertainty in the imbalance function the C_{dn} and C_{en} values are found to be in agreement with other studies for moderate to high wind speeds. These values increase very rapidly as U_{10n} decreases below 5 m/s. For the low wind speed range down to 0.1 m/s our study leads to very high drag coefficients. C_{dn} values are found to be higher by a factor of 10–100 compared to some other studies [*Cardone*, 1969] but are found to be in good agreement with *Greenhut and Khalsa* [1995] and YT96. The C_{en} values for heat fluxes also follow the same tendency, but the increase is not as great as for the C_{dn} at low wind speeds. These conclusions have been examined using sensitivity tests with regard to the imbalance for TKE transport terms, type of iterative algorithm (DB or DD), and inclusion of a free convection hypotheses. The qualitative increase of C_{dn} and C_{en} for U_{10n} decreasing from 5 to 0 m/s is maintained whatever the hypotheses.

Three different tests of the validity of the flux measurements at very low wind speeds have been undertaken. They concern the Taylor hypothesis of frozen turbulence, the shape of the spectral densities in the inertial subrange, and the hypothesis of local isotropy. All three analyses seem to validate the measurements, even at very low wind speeds. However, it should be mentioned that these validations of the inertial dissipation method at very low wind speed hold only in the context of shipboard measurements ensuring a minimum speed of 1 m/s for the sensors. However, there is some inconsistency in our analysis at the free convection limit. On one hand, our use of the inertial dissipation method assumes that the stress is aligned with the mean wind speed. On the other hand, the

discovery that the friction velocity is nearly constant for wind speeds below 3 m/s and tends toward an asymptotic value of 0.1 m/s is consistent with free convection considerations. That is, u^* is no longer a scaling parameter, and convection results in a nonzero wind stress. Further work is still needed for a better understanding of the inertial dissipation method at the free convection limit.

Acknowledgments. We wish to acknowledge the support of DRET (Direction de la Recherche et des Techniques), SHOM (Service Hydrographique et Océanographique de la Marine), DRED (Direction de la Recherche et des Etudes Doctorales), INSU (Institut National des Sciences de l'Univers du CNRS), Meteo-France/IFREMER (Institut Français de la Recherche sur la Mer), U.S. National Science Foundation, CNES (Centre National des Etudes Spatiales), and ASE (European Spatial Agency) in the SOFIA and the SEMAPHORE experiments. We wish to thank all the crew and the technical staff of the James Rennell Centre (England), University of Washington (Washington), CNET (Centre National d'Etudes des Telecommunications), CETP (Centre d'Etudes des Environnements Terrestres et Planétaires), and Meteo-France/CNRM (Centre National de Recherche en Météorologie) for their contribution to the campaigns. The James Rennell Centre contribution was partially funded by the Ministry of Agriculture, Fisheries, and Food.

References

Beljaars, A. C. M., The parametrization of surface fluxes in large scale models under free convection, *Tech. Memo. 215*, Res. Dep. of the Eur. Cent. for Medium-Range Weather Forecasts, Reading, England, 1995.

Boubnov, B. M., and G. S. Golitsyn, Temperature and velocity field regimes of convective motions in rotating plane fluid layer, *J. Fluid Mech.*, *219*, 215–239, 1990.

Bradley, E. F., P. A. Coppin, and J. S. Godfrey, Measurements of sensible and latent heat flux in the western equatorial Pacific Ocean, *J. Geophys. Res.*, *96*, 3375–3389, 1991.

Businger, J. A., A note on free convection, *Boundary Layer Meteorol.*, *4*, 323–326, 1973.

Cardone, V. J., Specification of the wind field distribution in the marine boundary layer for wave forecasting, *Tech. Rep. T.R. 69-1*, Geophys. Sci. Lab., New York Univ., New York, 1969.

Donelan, M. A., W. M. Drennan, and K. B. Katsaros, The air-sea momentum flux in conditions of wind sea and swell, *J. Phys. Oceanogr.*, in press, 1997.

Dupuis, H., A. Weill, K. B. Katsaros, and P. K. Taylor, Turbulent heat fluxes by profile and inertial dissipation methods: Analysis of the atmospheric surface layer from shipboard measurements during the SOFIA/ASTEX and SEMAPHORE experiments, *Ann. Geophys.*, *13*, 1065–1074, 1995.

Dyer, A. J., A review of flux-profile relationships, *Boundary Layer Meteorol.*, *7*, 363–372, 1974.

Edson, J. B., C. W. Fairall, P. G. Mestayer, and S. E. Larsen, A study of the inertial-dissipation method for computing air-sea fluxes, *J. Geophys. Res.*, *96*, 10,689–10,711, 1991.

Eymard, L., et al., Study of the air-sea interactions at the mesoscale: The SEMAPHORE experiment, *Ann. Geophys.*, *14*, 986–1015, 1996.

Fairall, C. W., and J. B. Edson, Recent measurements of the dimensionless turbulent kinetic energy dissipation function over the ocean, paper presented at Second International Conference on Air-Sea Interaction and on Meteorology and Oceanography of the Coastal Zone, Am. Meteorol. Soc., Lisbon, Portugal, Sept. 22–27, 1994.

Fairall, C. W., E. F. Bradley, D. P. Rogers, J. B. Edson, and G. S. Young, Bulk parameterization of air-sea fluxes for Tropical Ocean-Global Atmosphere Coupled-Ocean Atmosphere Response Experiment, *J. Geophys. Res.*, *101*, 3747–3764, 1996.

Foster, T. D., and S. Waller, Experiments on convection at very high Rayleigh numbers, *Phys. Fluids*, *28*(2), 455–461, 1985.

Frenzen, P., and C. A. Vogel, The turbulent kinetic energy budget in the atmospheric surface layer: A review and an experimental reexamination in the field, *Boundary Layer Meteorol.*, *60*, 49–76, 1992.

Gratchev, A. A., Free convection frequency spectra of atmospheric turbulence over the sea, *Boundary Layer Meteorol.*, *69*, 27–42, 1994.

Greenhut, G. H., and S. J. S. Khalsa, Bulk transfer coefficients and dissipation-derived fluxes in low wind speed conditions over the western equatorial Pacific Ocean, *J. Geophys. Res.*, *100*, 857–863, 1995.

Gurvich, A. S., and B. N. Yurchenko, Frequency spectra of temperature fluctuations in turbulent convection, *Izv. Acad. Sci. USSR Atmos. Oceanic Phys.*, Engl. Transl., *16*(8), 612–615, 1980.

Kader, B. A., Three-level structure of an unstably stratified atmospheric surface layer, *Izv. Acad. Sci. USSR Atmos. Oceanic Phys.*, Engl. Transl., *24*(12), 907–918, 1988.

Kader, B. A., Determination of turbulent momentum and heat fluxes by spectral methods, *Boundary Layer Meteorol.*, *61*, 323–347, 1992.

Kaimal, J. C., and J. E. Gaynor, Another look at sonic thermometry, *Boundary Layer Meteorol.*, *56*, 401–410, 1991.

Kaimal, J. C., J. C. Wyngaard, D. A. Haugen, O. R. Coté, Y. Izumi, S. J. Caughey, and C. J. Readings, Turbulence structure in the convective boundary layer, *J. Atmos. Sci.*, *33*, 2152–2168, 1976.

Large, W. G., and S. Pond, Open ocean momentum flux measurements in moderate to strong winds, *J. Phys. Oceanogr.*, *11*, 324–336, 1981.

Large, W. G., and S. Pond, Sensible and latent heat flux measurements over the ocean, *J. Phys. Oceanogr.*, *12*, 464–482, 1982.

Lenschow, D. H., Model of the height variation of the turbulent kinetic energy budget in the unstable planetary boundary layer, *J. Atmos. Sci.*, *31*, 465–474, 1974.

Lenschow, D. H., J. C. Wyngaard, and W. T. Pennell, Mean-field and second-moment budgets in a baroclinic, convective boundary layer, *J. Atmos. Sci.*, *37*, 1313–1326, 1980.

Neugum, A., Systematic influences in the determination of stress at sea with the so-called "dissipation" technique, Ph.D. thesis, Inst. für Meereskunde, Univ. zu Kiel, Kiel, Germany, 1996.

Nordeng, T. E., On the wave age dependent drag coefficient and roughness at sea, *J. Geophys. Res.*, *96*, 7167–7174, 1991.

Schumann, U., Minimum friction velocity and heat transfer in the rough surface layer of a convective boundary layer, *Boundary Layer Meteorol.*, *44*, 311–326, 1988.

Smith, S. D., Coefficients for sea surface wind stress, heat flux, and wind profiles as a function of wind speed and temperature, *J. Geophys. Res.*, *93*, 15,467–15,472, 1988.

Smith, S. D., et al., Sea surface wind stress and drag coefficients: The HEXOS results, *Boundary Layer Meteorol.*, *60*, 109–142, 1992.

Toba, Y., N. Lida, H. Kawamura, N. Ebuchi, and I. Jones, Wave dependence of sea surface wind stress, *J. Phys. Oceanogr.*, *20*, 705–721, 1990.

Weill, A., et al., SOFIA 1992 experiment during ASTEX, *Global Atmos. Ocean Syst.*, *3*, 355–395, 1995.

Wucknitz, J., The influence of anisotropy on stress estimation by the inertial dissipation method, *Boundary Layer Meteorol.*, *17*, 119–131, 1979.

Wyngaard, J., and O. Coté, The budgets of turbulent kinetic energy and temperature variance in the atmospheric surface layer, *J. Atmos. Sci.*, *28*, 190–201, 1971.

Yelland, M. J., and P. K. Taylor, Wind stress measurements from the open ocean, *J. Phys. Oceanogr.*, *26*, 541–558, 1996.

H. Dupuis and A. Weill, CETP/CNRS, 10-12 av. de l'Europe, 78140 Velizy, France. (e-mail: dupuis@geocean.u-bordeaux.fr; weill@cetp.ipsl.fr)

K. Katsaros, IFREMER, BP. 70, 29 280 Plouzané, France. (e-mail: Kristina.Katsaros@ifremer.fr)

P. K. Taylor, James Rennell Division for Ocean Circulation, Southampton Oceanography Centre, Southampton, S022 3ZH, England. (e-mail: Peter.K.Taylor@soc.soton.ac.uk)

(Received February 16, 1996; revised August 13, 1996; accepted January 3, 1997.)